Hypotony Maculopathy Obtained by Retro-mode Retinal Imaging.	Nakakura S, Okamoto A, Nagasato D, Tabuchi H, Kiuchi Y.	Ophthalmology.	2014	国外
Antimicrobial action from a novel porphyrin derivative in photodynamic antimicrobial chemotherapy in vitro.	Latief MA, Chikama T, Shibasaki M, Sasaki T, Ko JA, Kiuchi Y, Sakaguchi T, Obana A.	Lasers Med Sci	2014	国外
The whole macular choroidal thickness in subjects with primary open angle glaucoma.	Nakakura S, Yamamoto M, Terao E, Nagasawa T, Tabuchi H, Kiuchi Y	PLoS One.	2014	国外
Cross-sectional study of the association between a deepening of the upper eyelid sulcus-like appearance and wide-open eyes.	Nakakura S, Terao E, Nagatomi N, Matsuo N, Shimizu Y, Tabuchi H, Kiuchi Y	PLoS One. 29;9(4):e96249	2014	国外
Changes in angle of optic nerve and angle of ocular orbit with increasing age in Japanese children.	Tsukitome H, Hatsukawa Y, Morimitsu T, Yagasaki T, Kondo M.	Br J Ophthalmol.	2014	国外
RPE65 Mutations in Two Japanese Families with Leber Congenital Amaurosis.	Katagiri S, Hayashi T, Kondo M, Tsukitome H, Yoshitake K, Akahori M, Ikeo K, Tsuneoka H, Iwata T.	Ophthalmic Genet. 12:1-9	2014	国外
Changes in outer retinal microstructures during six month period in eyes with acute zonal occult outer retinopathy-complex.	Matsui Y, Matsubara H, Ueno S, Ito Y, Terasaki H, Kondo M.	PLoS One. 9:e110592	2014	国外

Whole exome analysis identifies frequent CNGA1 mutations in Japanese population with autosomal recessive retinitis pigmentosa.	Katagiri S, Akahori M, Sergeev Y, Yoshitake K, Ikeo K, Furuno M, Hayashi T, Kondo M, Ueno S, Tsunoda K, Shinoda K, Kuniyoshi K, Tsurusaki Y, Matsumoto N, Tsuneoka H, Iwata T.	PLoS One 9:e108721	2014	国外
Electroretinograms and level of aqueous vascular endothelial growth factor in eyes with hemicentral retinal vein occlusion or branch retinal vein occlusion.or branch retinal vein occlusion.	Yasuda S, Kachi S, Ueno S, Ushida H, Piao CH, Kondo M, Terasaki H	Jpn J Ophthalmol. 58:232-6.	2014	国外
The first USH2A mutation analysis of Japanese autosomal recessive retinitis pigmentosa patients: a totally different mutation profile with the lack of frequent mutations found in Caucasian patients	Zhao Y, Hosono K, Suto K, Ishigami C, Arai Y, Hikoya A, Hirami Y, Ohtsubo M, Ueno S, Terasaki H, Sato M, Nakanishi H, Endo S, Mizuta K, Mineta H, Kondo M, Takahashi M, Minoshima S,	J Hum Genet. 59 521-528	2014	国外
Clinical phenotype in ten unrelated Japanese patients with mutations in the EYS gene.	Suto K, Hosono K, Takahashi M, Hirami Y, Arai Y, Nagase Y, Ueno S, Terasaki H, Minoshima S, Kondo M, Hotta Y.	Ophthalmic Genet. 35 25-34	2014	国外
Interaction between optineurin and the bZIP transcription factor NRL.	Wang C-X, Hosono K, Ohtsubo M, Ohishi K. Gao J, Nakanishi N, Hikoya A, Sato M, Hotta Y, Minoshima S.	Cell Biol Int. 38 16-25	2014	国外

Oligomerization of optineurin and its oxidative stress- or E50K mutation-driven covalent cross-linking: possible relationship with glaucoma pathology.	Gao J, Ohtsubo M, Hotta Y, Minoshima S.	PLoS One 9, e101206	2014	国外
Efficacy of Short-term Postoperative Perfluoro-n-octane Tamponade for Pediatric Complex Retinal Detachment	Imaizumi A, Kusaka S, Noguchi H, Shimomura Y, Sawaguchi S.	Am J Ophthalmol. 157(2):384-389.	2014	国外
Combined treatment for Coats' disease: retinal laser photocoagulation combined with intravitreal bevacizumab injection was effective in two cases.	Kodama A, Sugioka K, Kusaka S, Matsumoto C, Shimomura Y.	BMC Ophthalmol. 25;14:36	2014	国外
Intravitreal injection of bevacizumab for retinopathy of prematurity.	Kuniyoshi K, Sugioka K, Sakuramoto H, Kusaka S, Wada N, Shimomura Y.	Jpn J Ophthalmol 58(3):237-43.	2014	国外
Fluorescein angiographic observations of peripheral retinal vessel growth in infants after intravitreal injection of bevacizumab as sole therapy for zone I and posterior zone II retinopathy of prematurity.	Tahija SG, Hersetyati R, Lam GC, Kusaka S, McMenamin PG.	Br J Ophthalmol. 98(4):507-12.	2014	国外
Intravitreal Injection of Bevacizumab for Retinopathy of Prematurity in an Infant with Peters Anomaly.	Minami T Kuniyoshi K, Kusaka S, Sugioka K Sakuramoto H, Sakamoto M, Izu A, Wada N, Shimomura Y	Case Rep Opthalmol 5:318-324	2014	国外

Genes to Cells

Derivation of human differential photoreceptor cells from adult human dermal fibroblasts by defined combinations of *CRX, RAX, OTX2* and *NEUROD*

Yuko Seko[1,2]*, Noriyuki Azuma[3], Toshiyuki Ishii[4], Yukari Komuta[1], Kiyoko Miyamoto[1], Yoshitaka Miyagawa[2], Makoto Kaneda[4] and Akihiro Umezawa[2]

[1]*Visual Functions Section, Department of Rehabilitation for Sensory Functions, Research Institute, National Rehabilitation Center for Persons with Disabilities, Tokorozawa, Saitama 359-8555, Japan*
[2]*Department of Reproductive Biology, Center for Regenerative Medicine, National Institute for Child Health and Development, Okura, Setagaya, Tokyo, 157-8535, Japan*
[3]*Department of Ophthalmology, National Center for Child Health and Development, Setagaya, Tokyo 157-8535, Japan*
[4]*Department of Physiology, Nippon Medical School, Sendagi, Bunkyo, Tokyo 113-8602, Japan*

Redirecting differentiation of somatic cells by over-expression of transcription factors is a promising approach for regenerative medicine, elucidation of pathogenesis and development of new therapies. We have previously defined a transcription factor combination, that is, *CRX, RAX* and *NEUROD*, that can generate photosensitive photoreceptor cells from human iris cells. Here, we show that human dermal fibroblasts are differentiated to photoreceptor cells by the same transcription factor combination as human iris cells. Transduction of a combination of the *CRX, RAX* and *NEUROD* genes up-regulated expression of the photoreceptor-specific genes, recoverin, blue opsin and PDE6C, in all three strains of human dermal fibroblasts that were tested. Additional *OTX2* gene transduction increased up-regulation of the photoreceptor-specific genes blue opsin, recoverin, S-antigen, CNGB3 and PDE6C. Global gene expression data by microarray analysis further showed that photoreceptor-related functional genes were significantly increased in induced photoreceptor cells. Functional analysis, that is, patch-clamp recordings, clearly revealed that induced photoreceptor cells from fibroblasts responded to light. Both the *NRL* gene and the *NR2E3* gene were endogenously up-regulated in induced photoreceptor cells, implying that exogenous *CRX, RAX, OTX2* and *NEUROD*, but not *NRL*, are sufficient to generate rod photoreceptor cells.

Introduction

Redirecting differentiation of somatic cells by over-expression of transcription factors is a promising approach for regenerative medicine, elucidation of pathogenesis and development of new therapies. The process is called 'direct reprogramming' or 'direct conversion' and has been shown in β cells, cardiomyocytes, neurons, platelets and photoreceptors. A specific combination of three transcription factors (Ngn3, Pdx1 and MafA) reprogram differentiated pancreatic exocrine cells in adult mice into cells that closely resemble beta cells (Zhou *et al.* 2008) and a combination of three factors (Gata4, Tbx5 and Baf60c) induce noncardiac mesoderm to differentiate directly into contractile cardiomyocytes (Takeuchi & Bruneau 2009). We recently employed the strategy of 'direct reprogramming' to generate retinal photoreceptor cells from human somatic cells, defining a combination of transcription factors, *CRX, RAX* and *NEUROD*, that induce light responsive photoreceptor cells (Seko *et al.* 2012). In that study, we induced 'iris cells' into photoreceptor cells. During vertebrate eye development, the inner layer of the optic cup differentiates into the

Communicated by: Takashi Tada
**Correspondence*: seko-yuko@rehab.go.jp

DOI: 10.1111/gtc.12127

neural retina and iris-pigmented epithelium (IPE). Therefore, the common developmental origin of the iris and the retina may make photoreceptor-induction from iris cells easier than from other types of somatic cells.

The induced pluripotent stem cells (iPS) developed by Takahashi and Yamanaka were the first model for 'direct reprogramming', in which mouse adult fibroblasts were reprogrammed by transduction of four transcription factor genes, Oct3/4, Sox2, c-Myc and Klf4 (Takahashi & Yamanaka 2006). Additionally, functional neurons were generated from mouse fibroblasts by a combination of three factors (Ascl1, Brn2 and Myt1 l) (Vierbuchen *et al.* 2010), and functional platelets were generated from mouse and human fibroblasts by a combination of three factors (p45NF-E2, MafG and MafK) (Ono *et al.* 2012). Because human dermal fibroblasts are less specialized than iris cells, we tested whether human dermal fibroblasts could be converted into photoreceptors by the same defined combination of genes used successfully for human iris cells, *CRX, RAX* and *NEUROD*, to generalize and establish our technology for 'generating photoreceptors'.

In this study, we also investigated an effect of additional transcription factor, *OTX2,* on transdifferentiation of somatic cells into retinal cells. Otx2 is essential for the cell fate determination of retinal photoreceptor cells (Nishida *et al.* 2003), and conditional disruption of the Otx2 gene decreases photoreceptor-associated genes (Omori *et al.* 2011).

Here, we show that the same combination of genes used for human iris cells, that is, *CRX, RAX and NEUROD*, generate human photoreceptor cells from human dermal fibroblasts, and that additional *OTX2* gene transduction further amplifies the expression of retina-specific genes. Our data therefore indicate that human dermal fibroblasts are a superior cell source for reprogramming into photoreceptor cells.

Results

Human dermal fibroblasts are induced into a rod- or cone-specific phenotype by defined transcription factors

We selected seven genes, *POU1F1*, *SOX2*, *PAX6*, *RAX*, *CRX*, *OTX2* and *NEUROD*, as candidate factors that may contribute to induce photoreceptor-specific phenotypes in human dermal fibroblasts, on the basis that such factors play a role in the development of photoreceptors. *CRX, RAX* and *NEUROD* are essential factors that induce photoreceptor cells from human iris cells (Seko *et al.* 2012) and *POU1f1,* Sox2 and Otx2 bind to the Rx promoter (Martinez-de Luna *et al.* 2010). Human dermal fibroblasts were infected with these genes and were examined for inducible expression of photoreceptor-specific genes. RT-PCR results showed that transduction of *CRX, RAX* and *NEUROD* (CRN) genes up-regulated the expression of the photoreceptor-specific genes recoverin, blue opsin and PDE6C, in all strains of fibroblasts tested (Fig. 1, panel A, B, C). Additionally, CRN-infected fibroblasts became positive for rhodopsin and blue opsin by immunohistochemistry (Fig. 1D). These results suggest that photoreceptor-specific phenotypes are induced by the same combination of transcription factors in human dermal fibroblasts as in human iris cells. However, it appeared that the combination of *CRX, RAX, NEUROD* and *OTX2* (CRNO) up-regulated the photoreceptor-specific blue opsin gene more strongly than the combination of CRN.

Additional *OTX2* gene transduction increases up-regulation levels of photoreceptor-specific genes

Expression levels of opsin- and phototransduction-related genes in induced- and noninduced fibroblasts were quantitated. Expression levels of S-antigen and recoverin, which are specifically expressed in rod photoreceptors, were much higher in CRNO-infected cells than in CRN-infected cells (S-antigen, $P < 0.01$, recoverin, $P < 0.05$; Welch's *t*-test, Fig. 2). In contrast, expression levels of rhodopsin, blue opsin, green opsin, recoverin, S-antigen, CNGB3 and PDE6C were not increased by additional *PAX6* gene infection (CRNP vs. CRN, in Fig. 2).

OTX2 is not an essential factor but an amplifier for induction of photoreceptor cells from human dermal fibroblasts

To investigate whether *OTX2* could be used as an alternative to the essential three genes, that is, *CRX, RAX* and *NEUROD*, we tested the effect of withdrawal of each individual factor from the four genes, that is, *CRX, RAX, NEUROD* and *OTX2*, on expression levels of the opsin- and phototransduction-related genes in induced photoreceptor cells (Fig. 3). Removal of either *CRX, RAX* or *NEUROD* resulted in a marked decrease in blue opsin, S-antigen, PDE6C

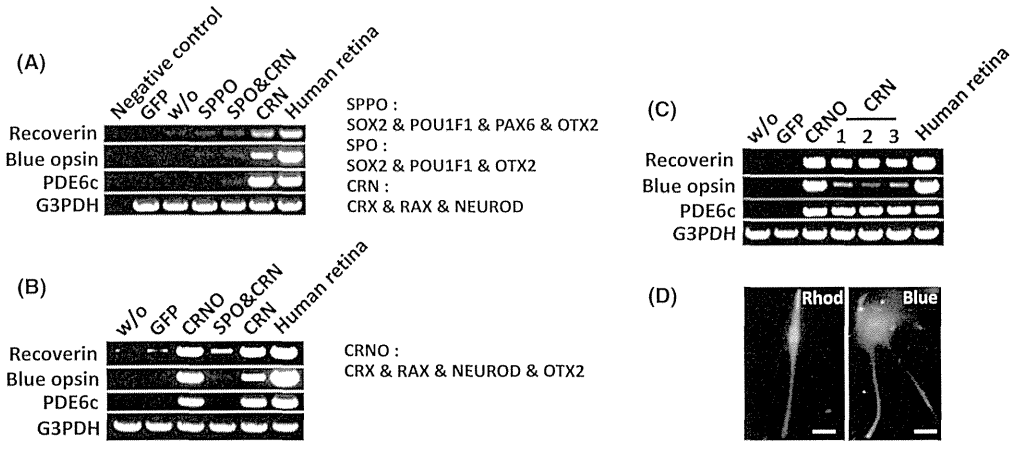

Figure 1 Induction of retina-specific genes in human dermal fibroblasts by the retroviral infection of genes for defined transcription factors. (A) RT-PCR analysis for photoreceptor-specific genes in cultured human dermal fibroblasts (NHDF) obtained from Lonza after gene transfer of several kinds of transcription factors. Recoverin, blue opsin and PDE6c genes were up-regulated by CRN transduction. 'Negative control': amplified water as a negative control. 'GFP': cultured fibroblasts after retroviral gene transfer of the GFP gene as another negative control. 'w/o': cultured fibroblasts without gene transfer as the other negative control. 'SPPO': *SOX2, POU1F1, PAX6* and *OTX2*. 'SPO': *SOX2, POU1F1* and *OTX2*. 'CRN': *CRX, RAX* and *NEUROD*. 'Human retina': human retinal tissue as a positive control. The amount of cDNA as a template was a half in the positive control. (B) RT-PCR analysis for photoreceptor-specific genes in cultured human dermal fibroblasts (NHDF) obtained from Promo Cell after gene transfer of several transcription factors. Recoverin, blue opsin and PDE6c genes were up-regulated by CRN or CRNO transduction. 'w/o': cultured fibroblasts without gene transfer as a negative control. 'GFP': cultured fibroblasts after retroviral gene transfer of the GFP gene as another negative control. 'CRNO': *CRX, RAX, NEUROD* and *OTX2*. (C) RT-PCR analysis for photoreceptor-specific genes in cultured human dermal fibroblasts (HDF-a) obtained from ScienCell after gene transfer of several transcription factors. Recoverin, blue opsin and PDE6C genes were up-regulated by CRN or CRNO transduction. Expression levels of blue opsin were increased by additional *OTX2* gene transduction. 'w/o': cultured fibroblasts without gene transfer as a negative control. 'GFP': cultured fibroblasts after retroviral gene transfer of the GFP gene as another negative control. 'CRNO': *CRX, RAX, NEUROD* and *OTX2*. '1', '2' and '3' mean independently cultured, transfected and harvested cells by the same combination of CRN genes. (D) Immunocytochemistry using antibodies to rhodopsin and blue opsin (green). Nuclei were stained with DAPI (blue). Experiments were carried out at 2 weeks after infection. The cells in the left panel and the right panel are CRN-infected Fib#2 and Fib#1, respectively. Scale bars represent 10 μm.

and CNGB3 levels; withdrawal of *RAX* resulted in a marked decrease in expression of blue opsin, and withdrawal of *NEUROD* resulted in a striking decrease in expression of PDE6C. Alternatively, withdrawal of *OTX2* alone did not affect the up-regulation of any of the tested photoreceptor-specific genes. These results indicate that *OTX2* is not an essential factor but an amplifier for induction of photoreceptor cells from human dermal fibroblasts, suggesting that additional *OTX2* plays a role in improving the balance and stability of photoreceptor-related gene expression in induced photoreceptor cells. Removal of either *CRX, RAX* or *NEUROD* resulted in a marked decrease in blue opsin, S-antigen, PDE6C and CNGB3 levels, suggesting that each transcription factor plays a role for specific molecular functions along with a role as a constituent of a combination for transdifferentiation to photoreceptor cells.

Photoreceptor-related functional genes are clearly up-regulated in induced photoreceptor cells from human dermal fibroblasts

To clarify the specific gene expression profile in induced photoreceptor cells, we compared the expression profiles of 50 599 probes in the induced photoreceptor cells (CRN-infected fibroblasts (CRN -Fib), CRNO-infected fibroblasts (CRNO-Fib) and parental cells [fibroblast (Fib)] by microarray analysis (uploaded to GEO accession #GPL16699 at http://www.ncbi.nlm.nih.gov/geo/index.cgi). We first extracted the intersection of the two groups of genes, that is, up-regulated genes by CRN-infection ([CRN-Fib] vs. [Fib]) and those by CRNO-infection ([CRNO-Fib] vs. [Fib]) (signal ratio $\geq +1.5$ for 'up'). According to gene ontology (GO) term annotation, the differentially expressed genes (4124 probes), which were

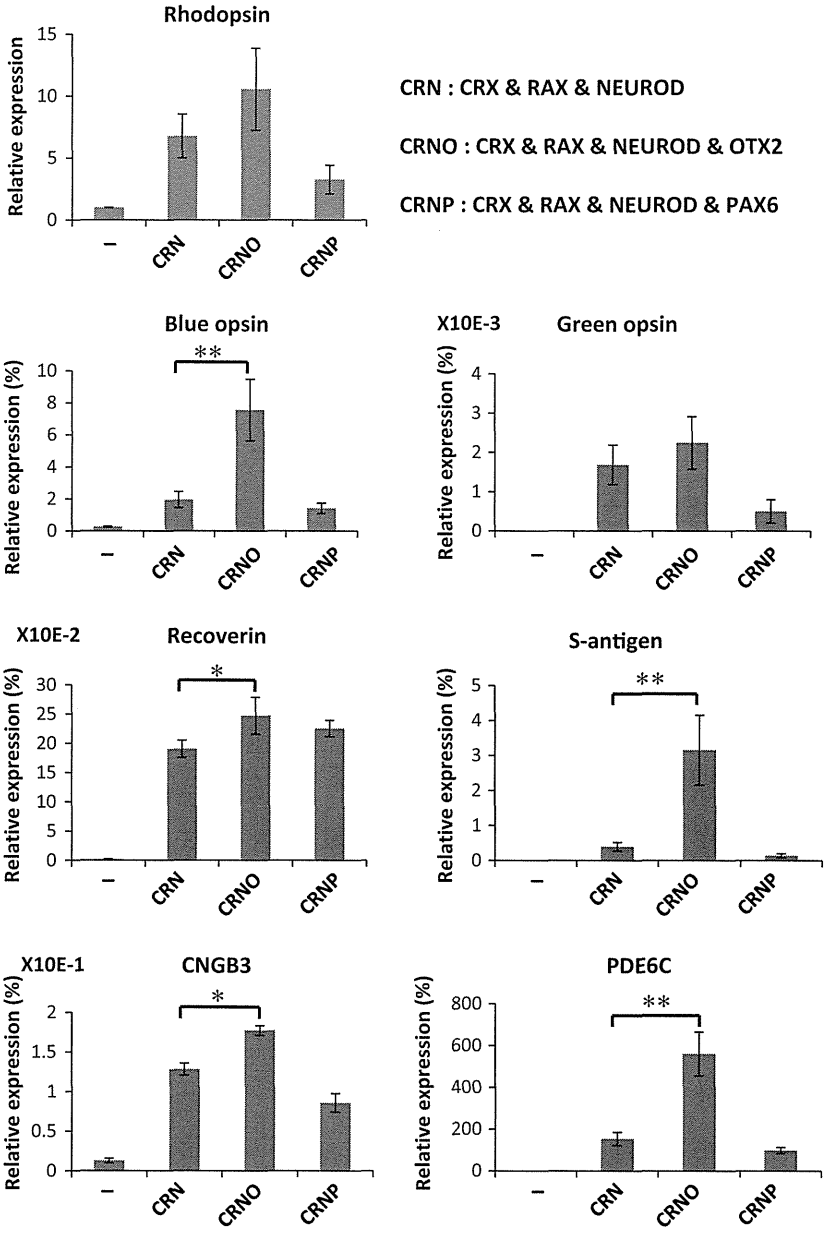

Figure 2 Effect of additional *OTX2* gene infection. Quantitative RT-PCR results for expression levels of rod- or cone-specific genes in induced photoreceptor cells from human dermal fibroblasts by the defined transcription factors. Quantitative expression levels of rhodopsin, blue opsin, green opsin, recoverin, S-antigen, CNGB3 and PDE6c genes were investigated. The data of green opsin, recoverin and CNGB3 were the results in experiments using Fib#2, and the data of rhodopsin, blue opsin and S-antigen were the results in experiments using Fib#3. The vertical axis indicates expression levels of each gene (%) in the indicated cells, relative to human retinal tissues. For rhodopsin, expression in cultured fibroblasts is regarded as 1.0. Results of statistical analyses for comparison of expression levels between CRNO-infected cells and CRN-infected cells are shown [$*P < 0.05$ and $**P < 0.01$ (Welch's *t*-test)]. '–': cultured fibroblasts without gene transfer as a negative control. 'CRN': *CRX, RAX* and *NEUROD*. 'CRNO': *CRX, RAX, NEUROD* and *OTX2*. 'CRNP': *CRX, RAX, NEUROD* and *PAX6*.

included in the intersection, were categorized into functional groups. Interestingly, when phototransduction-related genes were extracted, they accounted for up to 0.2% of the total (Fig. 4A; Table S1 in Supporting Information). In fact, signals of 16 probes were increased among the 30 phototransduction-related probes.

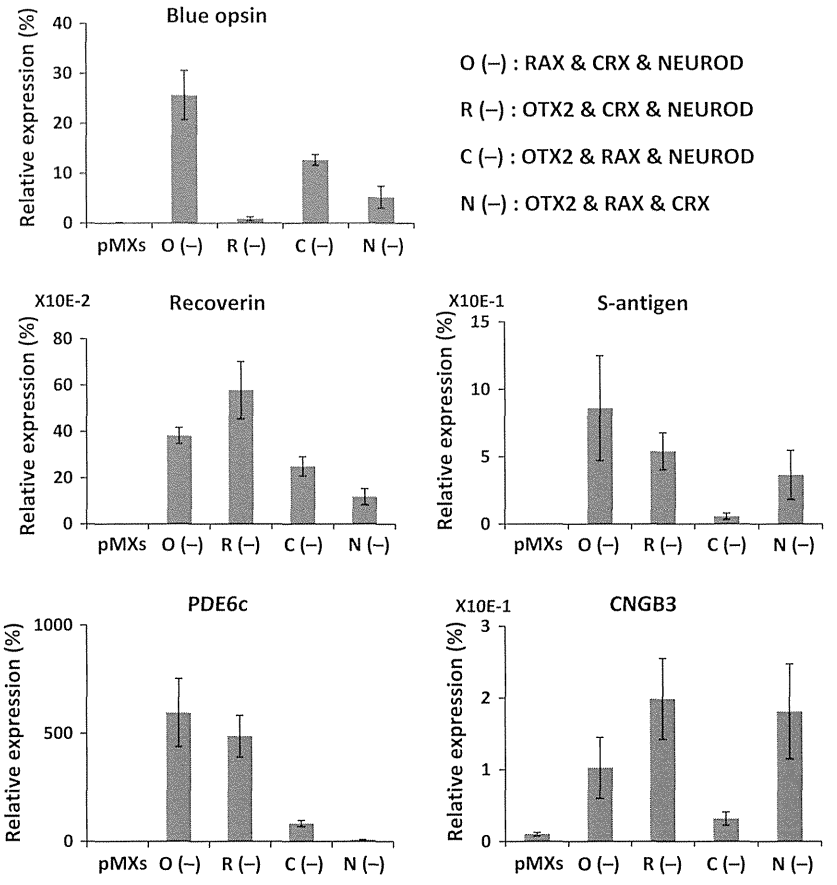

Figure 3 Effect of individual withdrawal of each gene from the combination of *CRX, RAX, NEUROD* and *OTX2*. Quantitative RT-PCR results for expression levels of rod- or cone-specific genes in induced photoreceptor cells from human dermal fibroblasts by the defined transcription factors. To determine which of the four genes, that is, *CRX, RAX, NEUROD* and *OTX2,* are critical, we examined the effect of withdrawal of individual factors from the pool of the candidate genes on expression of the opsin genes. In this experiment, Fib#3 was used. Quantitative expression levels of blue opsin, recoverin, S-antigen, CNGB3 and PDE6C genes were investigated. Vertical axis indicates expression levels of each gene (%) in the indicated cells, relative to human retinal tissues. Individual withdrawal of *RAX* resulted in a significant decrease in expression of blue opsin and withdrawal of *CRX* resulted in a significant decrease in S-antigen PDE6C and CNGB3. Individual withdrawal of *NEUROD* resulted in a significant decrease in PDE6C. However, withdrawal *OTX2* could up-regulate all of the retina-specific genes tested. 'O(-)': *CRX, RAX* and *NEUROD*. 'R(-)': *CRX, OTX2* and *NEUROD*. 'C(–)': *OTX2, RAX* and *NEUROD*. 'N(-)': *CRX, RAX* and *OTX2*. 'pMXs': cultured fibroblasts after retroviral gene transfer of the pMXs gene as a negative control.

To clarify the difference in gene expression profiles between fibroblast-derived and iris-derived photoreceptor cells, we investigated the expression profiles of default cells (iris cells) and induced cells (CRN-infected iris cells). We carried out GO analysis based on the differentially expressed genes (2585 probes), which were included in the commonly up-regulated genes, that is, ([CRNO-Fib] vs. [Fib]) and ([CRN-Iris] vs. [Iris]) (signal ratio $\geq +1.5$ for 'up'). The phototransduction-related genes were extracted and accounted for up to 4.4% (Fig. 4B; Table S2 in Supporting Information). Although detection/perception, which includes detection of external stimulus, detection of abiotic stimulus and detection of light stimulus, accounted for up to 0.6% of the total in Fig. 4A, the detection/perception accounted for up to 21.1% in Fig. 4B.

A dermal fibroblast could be a cell source as well as an iris cell

We searched up-regulated genes both in the CRNO-infected fibroblasts and in CRN-infected iris cells (signal ratio ≥ 2.0 for 'up') and named as 'intersection

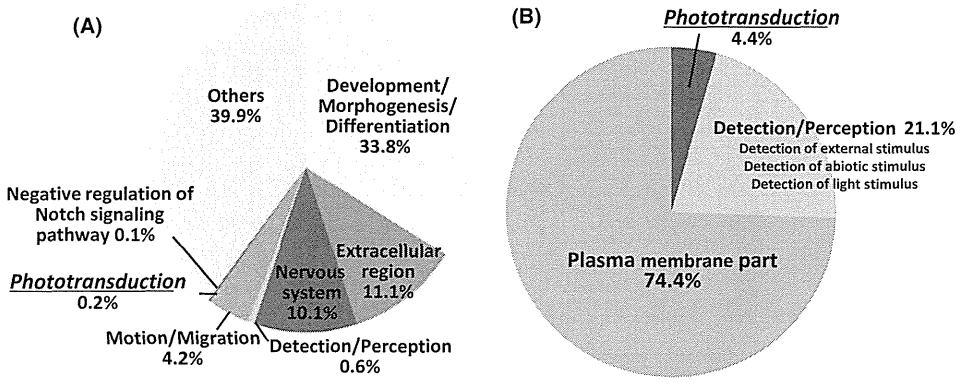

Figure 4 Categorization of the genes differentially expressed in induced photoreceptor cells from human dermal fibroblasts by the defined transcription factors. (A) Categorization of commonly up-regulated genes in induced photoreceptor cells from human dermal fibroblasts by genes transduction of CRN and CRNO. To clarify the specific gene expression profile in induced photoreceptor cells, we compared the expression levels of 50 599 probes in the induced photoreceptor cells (CRN-infected fibroblasts (CRN-Fib), CRNO-infected fibroblasts (CRNO-Fib) and parental cells [fibroblast (Fib)] by microarray analysis. We searched up-regulated genes in the induced photoreceptor cells by CRN- and CRNO-infection compared with parental cells (signal ratio $\geq +1.5$ for 'up'), respectively. We then extracted the intersection of the two groups of genes, that is, up-regulated genes by CRN-infection and those by CRNO-infection. According to gene ontology (GO) term annotation, the genes differentially expressed in the induced photoreceptor cells by CRN- and CRNO-infection (4124 probes) were categorized into functional group, figuring out the relative importance or significance of the GO-term [corrected P-value < 0.01)]. After that, we carried out additional categorization into eight groups. Interestingly, phototransduction-related genes were extracted and account for up to 0.15% of the total. (B) Categorization of commonly up-regulated genes (2585 probes) in the CRNO-transfected dermal fibroblasts and CRN-transfected iris cells (signal ratio ≥ 1.5 for 'up'). According to gene ontology (GO) term annotation, the genes differentially expressed in the induced photoreceptor cells (2585 probes) were categorized into functional groups to figure out the relative importance or significance of the GO term (corrected P-value < 0.01).

of Fib and Iris'. Then, we extracted retina-related genes from them according to Gene Ontology and a previous paper (Omori *et al.* 2011). We focused on remarkably up-regulated genes ([CRNO-Fib]/[Fib] > 9.0) and extracted them (Fig. 5A). We then compared signal ratios between [CRNO-Fib]/[Fib] (ΔFib) and [CRN-Iris]/[Iris] (ΔIris). The signal ratios of 18 probes were higher in [CRNO-Fib] (ΔFib/ΔIris $\geq$ 2.0); however, the signal ratios of 47 signals were higher in [CRN- Iris] (ΔIris/ΔFib $\geq$ 2.0). As for other 78 probes, the signal ratios were regarded not to be significantly different (Fig. 5B; Table S3 in Supporting Information). To analyze the gene expression data in an unsupervised manner, we carried out principal component analysis (PCA). The gene expression patterns in the CRN-Fib, CRNO-Fib and CRN-Iris were close based on component 2 (PC2) but were apart from the parent cells (Fib and Iris) (Fig. 5C). We investigated the difference in endogenous expression of *CRX, RAX* and *NEUROD* between CRN-Fib and CRN-iris by RT-PCR (Fig. 5D). The endogenous *CRX* genes started to be expressed in CRN-Fib, but the expression levels of *RAX* and *NEUROD* were higher in CRN-Iris than in CRN-Fib. Both the *NRL* gene and the *NR2E3* gene were endogenously up-regulated in the induced photoreceptor cells, that is, CRN-Fib, CRNO-Fib and CRN-Iris (Fig. 5E).

Induced photoreceptor cells from fibroblasts are photoresponsive *in vitro*

Light stimulation was applied to infected or non-infected human fibroblasts because CRN- or CRNO-infected cells showed the photoreceptor-like phenotypes by RT-PCR and global gene expression analyses. Among cells tested, significant light responses were detected in a portion of infected cells (Fig. 5F; Fig. S2 in Supporting Information). An infected cell presented a large outward current when exposed to light (Fig. 5F, upper panel). However, no detectable outward current was evoked when light stimulation was given to a noninfected cell (Fig. 5F, lower panel).

Discussion

This is the first report that human dermal fibroblasts can differentiate into photoreceptor cells by the same combination of transcription factors, *CRX, RAX* and

(A) **Remarkably up-regulated genes in induced photoreceptor cells.**

ProbeName	GeneSymbol	GeneName	Fib	Induced-Fib	Iris	Induced-Iris
A_23_P5853	SAG	S-antigen; retina and pineal gland (arrestin)	9.06	532.20	8.07	269.06
A_24_P165423	RBP7	Retinol binding protein 7, cellular	8.99	509.01	3.91	15.04
A_23_P202427	HKDC1	Hexokinase domain containing 1	8.25	303.69	6.67	101.72
A_32_P64200	GUCA1B	Guanylate cyclase activator 1B (retina)	6.82	112.66	5.64	49.88
A_23_P81825	GUCA1B	Guanylate cyclase activator 1B (retina)	6.47	88.71	6.10	68.64
A_23_P7402	PDZD2	PDZ domain containing 2	6.31	79.58	4.35	20.38
A_24_P355626	ABCG4	ATP-binding cassette, sub-family G (WHITE), member 4	6.02	64.86	1.57	2.97
A_33_P3409944	GNAT2	Guanine nucleotide binding protein (G protein)	5.93	60.92	3.90	14.90
A_23_P98070	PDE6C	Phosphodiesterase 6C, cGMP-specific, cone	5.71	52.17	5.62	49.10
A_23_P81590	PDE6A	Phosphodiesterase 6A, cGMP-specific, rod, alpha	7.19	146.24	9.12	556.79
A_33_P3232290	NPS	Neuropeptide S	5.98	63.21	9.05	528.87
A_33_P3338631	NRL	Neural retina leucine zipper	5.94	61.51	8.37	329.70
A_23_P325562	SLC1A7	Solute carrier family 1 (glutamate transporter), member 7	8.05	265.79	8.05	265.14
A_23_P88278	RPGRIP1	Retinitis pigmentosa GTPase regulator interacting protein 1	7.71	209.81	8.02	260.12
A_23_P40856	LRTM1	Leucine-rich repeats and transmembrane domains 1	6.61	97.79	8.01	257.16
A_23_P351305	FAM123A	Family with sequence similarity 123A	6.62	98.12	7.62	196.86
A_23_P76350	GNB3	Guanine nucleotide binding protein (G protein), beta polypeptide 3	5.94	61.28	5.96	62.17

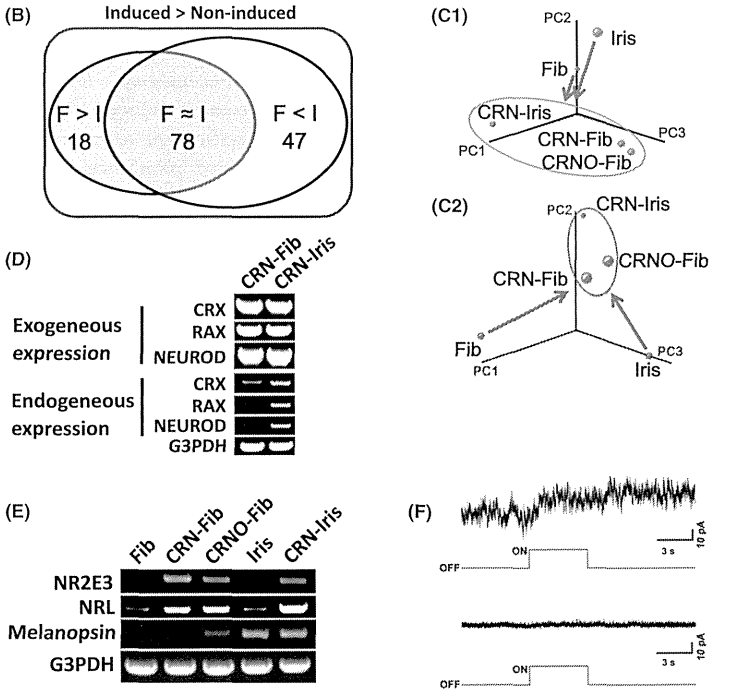

Figure 5 Comparison of gene expression profiles of up-regulated genes in induced photoreceptor cells from dermal fibroblasts and from iris cells. (A) Remarkably up-regulated genes in induced photoreceptor cells ([CRNO-Fib]/[Fib] > 9.0). (B) Microarray analysis data sets from up-regulated genes in induced photoreceptor cells from dermal fibroblasts and from iris cells. F > I: Signal ratio of F/signal ratio of I ≥ 2.0. F < I: Signal ratio of I/signal ratio of F ≥ 2.0. The numbers of probes in each category are indicated. (C) Three-dimensional representation of PCA of gene expression levels (C-1: PCA based on the expression of all genes. C-2: PCA based on the expression of retina-related genes). It was shown that CRN-Fib, CRNO-Fib and CRN-Iris were grouped into the same group (shown in circle), suggesting that genes expression patterns in the CRN-Fib, CRNO-Fib and CRN-Iris were similar based on component 2 (PC2) and were apart from parent cells (Fib and Iris). (D) RT-PCR analysis of the exogenous and endogenous genes in induced retinal cells. Expression of the *CRX, RAX* and *NEUROD* and genes in the transgene-induced cells was analyzed by RT-PCR, using the exogenous and endogenous gene-specific primers (Seko *et al.* 2012). Equal amounts of RNAs were examined as determined by normalization by expression of the G3PDH gene. The levels of endogenous genes expression of *CRX, RAX* and *NEUROD* were clearly higher in CRN-Iris than in CRN-Fib. (E) RT-PCR analysis of genes expression of the transcription factor, *NRL* and *NR2E3*, and melanopsin. Expression of *NRL* and *NR2E3* was clearly up-regulated in the transgene-induced cells. The combination of CRN may be sufficient to up-regulate those transcription factors genes. As for melanopsin, expression was detected in CRNO-fib, but not in Fib or CRN-Fib. By microarray analysis, any expression of melanopsin was not detected (uploaded to GEO accession #GPL16699 at http://www.ncbi.nlm.nih.gov/geo/index.cgi). (F) Responses to light in infected cells and noninfected cells. Responses to light in infected cells (upper panel) and noninfected cells (lower panel). In a CRNO-infected cell (Fib #2), there was a large outward current when cell was exposed to light (upper panel). However, no detectable outward current was evoked when light stimulation was given to a noninfected cell (lower panel). A timing and duration of light stimulation is shown under the current trace. Holding potential was 0 mV.

NEUROD (Seko *et al.* 2012), that were used successfully for iris cells (Fig. 1). An additional gene added to the combination, *OTX2*, further increases expression levels of photoreceptor-specific genes (Fig. 2). Global gene expression data by microarray analysis further shows that photoreceptor-related functional genes are significantly increased in induced photoreceptor cells (Fig. 4). Our data suggest that *OTX2* plays a role as an amplifier of photoreceptor-related functions (Figs 2 and 3; Fig. S1 in Supporting Information). Functional analysis also revealed that induced photoreceptor cells from fibroblasts by *CRX, RAX, NEUROD* and *OTX2* are photoresponsive *in vitro* (Figs 5F; Fig. S2 in Supporting Information).

Dermal fibroblasts are of mesodermal origin and immunogenic, whereas iris-pigmented epithelial cells (IPE cells) are of neural ectoderm-origin and show immune tolerance. Iris cells studied here include not only IPE cells but also iris stromal cells, which are of neural crest origin. We have previously shown that iris cells, IPE cells and iris stromal cells are differentiated into photoreceptor cells in the same way (Seko *et al.* 2012). However, dermal fibroblasts are harvested easily and safely, and iris cells are obtained surgically. To find a more suitable cell source than the iris cells for reprogramming into photoreceptor cells, we compared signal ratios between CRNO-Fib and CRN-Iris by a microarray analysis. The results show that there is an increase in both the expression levels and the variety of up-regulated photoreceptor-specific genes in induced cells from iris when compared with dermal fibroblasts (Fig. 5B; Table S3 in Supporting Information). From the standpoint of regenerative medicine, iris cells may be more suitable than dermal fibroblasts based on their characteristics of immune tolerance and higher expression of retina-specific genes in differentiated cells. The difference in induced endogenous expression of transcription factors *CRX, RAX* and *NEUROD* between CRN-Fib and CRN-Iris as well as the difference in up-regulated photoreceptor-specific genes may suggest a difference in reprogramming potential between the human dermal fibroblasts and the human iris cells (Fig. 5C). It may be possible to improve dermal fibroblasts as a source by use of other transcription factors or manipulating the histone methylation signature (Bramswig *et al.* 2013). However, dermal fibroblasts have an important advantage in that these cells are obtained safely and easily from patients. Because the direct reprogramming method may be suitable to provide the small numbers of cells required for individualized drug screening and disease modeling, dermal fibroblasts may be useful for such purposes despite their limitations.

We have previously shown that the combination of *CRX* and *NEUROD*, but not *NRL*, is sufficient for rod-specific gene expression (Seko *et al.* 2012), but Mears *et al.* (2001) reported that *Nrl* is necessary for rod-photoreceptor development. The present study indicates that both the *NRL* gene and the *NR2E3* gene are endogenously up-regulated in induced photoreceptor cells (CRNO-Fib and CRN-Iris) by microarray analyses and RT-PCR (Fig. 5D; Table S3 in Supporting Information). Endogenous NRL expression by the three factors, *CRX, RAX* and *NEUROD*, may promote retinal differentiation in the absence of the exogenous *NRL* gene. This fact clearly shows that exogenous gene transduction of the combination, *CRX, RAX* and *NEUROD*, is sufficient but *NRL* is not essential to induce rod photoreceptor-specific gene expression.

Several retinal diseases, including retinitis pigmentosa (RP), age-related macular degeneration and cone dystrophy, lead to loss of vision, due to loss of photoreceptors and retinal pigment epithelium (RPE), especially, RP leads to visual impairment due to irreversible retinal degeneration, which is determined genetically in most cases. Gene therapy has been implicated for Leber's congenital amaurosis (Bainbridge *et al.* 2008). Another promising therapeutic strategy is to transplant functional photoreceptor cells and retinal pigment epithelial cells. Sheets of human fetal neural retina with retinal pigment epithelium (Radtke *et al.* 2004) and ES cell-derived photoreceptors (Osakada *et al.* 2008) have been implicated for use as sources for the photoreceptor cells. The technology for producing retinal sheets from ES cell/iPSCs by self-organogenesis (Eiraku *et al.* 2011) is promising for retinal transplantation. Recently, Tanaka *et al.* (2013) reported that inducible expression of myogenic differentiation 1 (*MYOD1*) in immature human iPSCs drives cells along the myogenic lineage, with efficiencies reaching 70–90%. Although induction of human neural retina takes a long time (Nakano *et al.* 2012), there is a possibility that the induction period could be shortened by the aid of the defined factors that we determined. We have previously reported the defined combination of transcription factors, that is, *CRX, RAX* and *NEUROD*, induce light-responsive photoreceptor cells in humans using iris cells (Seko *et al.* 2012). We show here the function of the *OTX2* gene as an amplifier of retinal transdifferentiation of human dermal fibroblasts (Figs 2 and 3; Fig. S1 in Supporting Information). In

conclusion, *OTX2* and the three transcription factors, *CRX*, *RAX* and *NEUROD*, are promising as tools for effective retinal induction.

Experimental procedures

Cell culture

Three strains of cultured human dermal fibroblasts were used: one was obtained from Lonza (NHDF), another was from Promo Cell (NHDF) and the other was from ScienCell (HDF-a). These three kinds of fibroblasts were designated as Fib#1, Fib#2 and Fib#3, respectively. The cells were cultured in the recommended medium by the manufactures (FGM-2 Bullet kit, Fibroblast Growth Medium Kit, and Fibroblast Medium, respectively). Iris cells were obtained as previously reported (Seko *et al.* 2012) with the approval (approval number, #156) of the Ethics Committee of the National Institute for Child and Health Development (NCCHD), Tokyo. The ethics committees of the NCCHD and National Rehabilitation Center for Persons with Disabilities specifically approved this study. Signed informed consent was obtained from donors, and the surgical specimens were irreversibly de-identified. All experiments handling human cells and tissues were carried out in line with the Tenets of the Declaration of Helsinki. The iris cells were cultured in the growth medium [Dulbecco's modified Eagle's medium (DMEM)/Nutrient mixture F12 (1:1) supplemented with 10% fetal bovine serum, insulin–transferrin–selenium, and MEM-NEAA (GIBCO)].

Preparation and infection of recombinant retrovirus

Full-length transcription factors, *SOX2* (Martinez-de Luna *et al.* 2010), *POU1F1* (Martinez-de Luna *et al.* 2010), *OTX2* (Nishida *et al.* 2003), *PAX6* (Glaser *et al.* 1992), *RAX* (Mathers *et al.* 1997), *CRX* (Furukawa *et al.* 1997) and *NEUROD* (Morrow *et al.* 1999), were amplified from cDNAs prepared from total RNA of adult human retina (Clontech, CA, USA) by PCR and cloned into the XmnI-EcoRV sites of pENTR11 (Invitrogen). Each vector contained one transcription factor, and a mixture of vectors was used.

Preparation and infection of recombinant retrovirus were carried out as previously reported (Seko *et al.* 2012). In brief, the resulting pENTR11-transcription factors were recombined with pMXs-DEST by use of LR recombination reaction as instructed by the manufacturer (Invitrogen). The retroviral DNAs were then transfected into 293FT cells, and 3 days later, the media were collected and concentrated. The human dermal fibroblasts and the iris cells were infected with this media containing retroviral vector particles. After the retroviral infection, the media were replaced with the DMEM/F12/B27 medium supplemented with 40 ng/ml bFGF, 20 ng/ml EGF, fibronectin and 1% FBS. The retrovirus-infected cells were cultured for up to 14 days. We transfected retroviral eGFP under the same condition to measure efficiency of infection. The frequency of eGFP-positive cells was 90–94% of all cells at 48 h after infection.

Reverse transcriptase-PCR

Total RNA was isolated with an RNeasy Plus mini-kit® (Qiagen, Maryland, USA) or PicoPure™ RNA Isolation Kit (Arcturus Bioscience, CA, USA) according to the manufacturer's instruction. An aliquot of total RNA was reverse transcribed using an oligo (dT) primer. The design of PCR primer sets is shown in our previous paper (Seko *et al.* 2012).

Quantitative RT-PCR

cDNA template was amplified (ABI7900HT Sequence Detection System) using the Platinum Quantitative PCR SuperMix-UDG with ROX (11743-100, Invitrogen). Fluorescence was monitored during every PCR cycle at the annealing step. The authenticity and size of the PCR products were confirmed using a melting curve analysis (using software provided by Applied Biosystems) and a gel analysis. A mRNA level was normalized using G3PDH as a housekeeping gene. The design of PCR primer sets is shown in our previous paper (Seko *et al.* 2012).

Immunocytochemistry

Immunocytochemical analysis was carried out as previously described (Kohyama *et al.* 2001). As a methodological control, the primary antibody was omitted. The primary antibodies used were as follows: rhodopsin (goat polyclonal, I-17, Santa Cruz) and blue opsin (goat polyclonal, P-13, Santa Cruz).

Global gene expression analysis

To clarify the specific gene expression profile in induced photoreceptor cells, we compared the expression levels of 50 599 probes in the induced photoreceptor cells and parental cells using the SurePrint G3 Human Gene Expression Microarray 8 × 60 K, ver.2.0 (Agilent) using total RNA extracted from those cells. To average experimental variations, extracted total RNA samples were pooled into one tube from three independent induction experiments of human dermal fibroblasts (Fib#2) and 12 independent induction experiments of human iris cells, respectively, and pooled samples were served to microarray analyses. To normalize the variations in staining intensity among chips, the 75th percentile of intensity distributions was aligned across arrays using GeneSpring software, version 12.5 (Agilent Technologies, Palo Alto). We then carried out GO analysis based on the normalized expression data of induced and noninduced cells. Commonly up-regulated genes in CRN- and CRNO-transfected fibroblasts (4124 probes) and those in CRNO-transfected fibroblasts and CRN-transfected iris cells (2585 probes) were extracted and were catego-

rized into functional groups, respectively, to figure out the relative importance or significance of the gene ontology (GO) term (corrected P-value < 0.01). To analyze and compare the gene expression data of the induced cells and parent cells in an unsupervised manner, we used principal component analysis (PCA).

Light stimulation and electrophysiological recordings

We followed the method in our previous paper (Seko *et al.* 2012). Briefly, a high pressure UV lamp (USH-102D, Ushio) was used as a light source. Diffuse, unpolarized blue light was generated through bandpass filters attached with the fluorescent emission system (BX-FLA, Olympus, Tokyo, Japan). Wavelength of light for stimulation was 460–490 nm. Duration and timing of light stimulation was controlled by an electrically controlled shutter attached to the UV lamp box. The trigger signals to the electrically controlled shutter were given by commercially available software (pClamp 9) through AD/DA. Light intensity used for stimulation was 390 W/m^2. To activate the phototransduction cascade, 11-*cis* retinal (a gift from the vision research community, the National Eye Institute, National Institutes of Health) was added to the culture medium of human fibroblasts to a concentration of 37.5 μM with 0.15% ethanol as a vehicle, approximately 45 min before the electrical recording. Electrical recordings were made in the whole-cell patch-clamp configuration. The composition of the intrapipette solution was (in mM) KCl, 135; $CaCl_2$, 0.5; HEPES, 5; EGTA, 5; ATP-2Na, 5; GTP-3Na, 1; and pH was adjusted to 7.3 with KOH. The resistance of patch pipettes was 12–15 MΩ when filled with an intrapipette solution. The membrane current was recorded with a patch-clamp amplifier (Axopatch-200B; Axon Instruments, Foster City, CA, USA), low-pass filtered with a cutoff frequency of 1 kHz and digitized at 2 kHz through a DigiData 1322A Interface using pCLAMP software (version 8.0, Axon Instruments). We recorded light responses from noninfected cells, CRN-infected cells and CRNO-infected cells. Recorded data were pooled for further analysis (for details, see Fig. S2 in Supporting Information).

Acknowledgements

We are grateful for the National Eye Institute, National Institutes of Health for gift of 11-*cis* retinal, S. Kato, K. Mori, S. Toyama and Y. Takahashi for the support throughout the work and for H. Miyauchi for the technical assistance. This research was supported by grants from the Ministry of Education, Culture, Sports, Science, and Technology (MEXT) of Japan, by Ministry of Health, Labour and Welfare Sciences (MHLW) research grants, by a Research Grant on Health Science focusing on Drug Innovation from the Japan Health Science Foundation, by the program for the promotion of Fundamental Studies in Health Science of the Pharmaceuticals and Medical Devices Agency, by the Grant of National Center for Child Health and Development to AU, by the Nippon Medical School Grant-in-Aid for Medical Research to MK and by grants of National Rehabilitation Center for Persons with Disabilities.

Author contributions

YS carried out all of the experiments; MK, TI, YS, YK carried out electrophysiological analyses; YS, YM and KM prepared viral vectors; YS, NA, AU made experimental designs; and YS and AU wrote the manuscript.

References

Bainbridge, J.W., Smith, A.J., Barker, S.S. *et al.* (2008) Effect of gene therapy on visual function in Leber's congenital amaurosis. *N. Engl. J. Med.* **358**, 2231–2239.

Bramswig, N.C., Everett, L.J., Schug, J., Dorrell, C., Liu, C., Luo, Y., Streeter, P.R., Naji, A., Grompe, M. & Kaestner, K.H. (2013) Epigenomic plasticity enables human pancreatic alpha to beta cell reprogramming. *J. Clin. Invest.* **123**, 1275–1284.

Eiraku, M., Takata, N., Ishibashi, H., Kawada, M., Sakakura, E., Okuda, S., Sekiguchi, K., Adachi, T. & Sasai, Y. (2011) Self-organizing optic-cup morphogenesis in three-dimensional culture. *Nature* **472**, 51–56.

Furukawa, T., Morrow, E.M. & Cepko, C.L. (1997) Crx, a novel otx-like homeobox gene, shows photoreceptor-specific expression and regulates photoreceptor differentiation. *Cell* **91**, 531–541.

Glaser, T., Walton, D.S. & Maas, R.L. (1992) Genomic structure, evolutionary conservation and aniridia mutations in the human PAX6 gene. *Nat. Genet.* **2**, 232–239.

Kohyama, J., Abe, H., Shimazaki, T., Koizumi, A., Nakashima, K., Gojo, S., Taga, T., Okano, H., Hata, J. & Umezawa, A. (2001) Brain from bone: efficient "meta-differentiation" of marrow stroma-derived mature osteoblasts to neurons with Noggin or a demethylating agent. *Differentiation* **68**, 235–244.

Martinez-de Luna, R.I., Moose, H.E., Kelly, L.E., Nekkalapudi, S. & El-Hodiri, H.M. (2010) Regulation of retinal homeobox gene transcription by cooperative activity among cis-elements. *Gene* **467**, 13–24.

Mathers, P.H., Grinberg, A., Mahon, K.A. & Jamrich, M. (1997) The Rx homeobox gene is essential for vertebrate eye development. *Nature* **387**, 603–607.

Mears, A.J., Kondo, M., Swain, P.K., Takada, Y., Bush, R.A., Saunders, T.L., Sieving, P.A. & Swaroop, A. (2001) Nrl is required for rod photoreceptor development. *Nat. Genet.* **29**, 447–452.

Morrow, E.M., Furukawa, T., Lee, J.E. & Cepko, C.L. (1999) NeuroD regulates multiple functions in the developing neural retina in rodent. *Development* **126**, 23–36.

Nakano, T., Ando, S., Takata, N., Kawada, M., Muguruma, K., Sekiguchi, K., Saito, K., Yonemura, S., Eiraku, M. & Sasai, Y. (2012) Self-formation of optic cups and storable stratified neural retina from human ESCs. *Cell Stem Cell* **10**, 771–785.

Nishida, A., Furukawa, A., Koike, C., Tano, Y., Aizawa, S., Matsuo, I. & Furukawa, T. (2003) Otx2 homeobox gene controls retinal photoreceptor cell fate and pineal gland development. *Nat. Neurosci.* **6**, 1255–1263.

Omori, Y., Katoh, K., Sato, S., Muranishi, Y., Chaya, T., Onishi, A., Minami, T., Fujikado, T. & Furukawa, T. (2011) Analysis of transcriptional regulatory pathways of photoreceptor genes by expression profiling of the Otx2-deficient retina. *PLoS ONE* **6**, e19685.

Ono, Y., Wang, Y., Suzuki, H., Okamoto, S., Ikeda, Y., Murata, M., Poncz, M. & Matsubara, Y. (2012) Induction of functional platelets from mouse and human fibroblasts by p45NF-E2/Maf. *Blood* **120**, 3812–3821.

Osakada, F., Ikeda, H., Mandai, M., Wataya, T., Watanabe, K., Yoshimura, N., Akaike, A., Sasai, Y. & Takahashi, M. (2008) Toward the generation of rod and cone photoreceptors from mouse, monkey and human embryonic stem cells. *Nat. Biotechnol.* **26**, 215–224.

Radtke, N.D., Aramant, R.B., Seiler, M.J., Petry, H.M. & Pidwell, D. (2004) Vision change after sheet transplant of fetal retina with retinal pigment epithelium to a patient with retinitis pigmentosa. *Arch. Ophthalmol.* **122**, 1159–1165.

Seko, Y., Azuma, N., Kaneda, M., Nakatani, K., Miyagawa, Y., Noshiro, Y., Kurokawa, R., Okano, H. & Umezawa, A. (2012) Derivation of human differential photoreceptor-like cells from the iris by defined combinations of CRX, RX and NEUROD. *PLoS ONE* **7**, e35611.

Takahashi, K. & Yamanaka, S. (2006) Induction of pluripotent stem cells from mouse embryonic and adult fibroblast cultures by defined factors. *Cell* **126**, 663–676.

Takeuchi, J.K. & Bruneau, B.G. (2009) Directed transdifferentiation of mouse mesoderm to heart tissue by defined factors. *Nature* **459**, 708–711.

Tanaka, A., Woltjen, K., Miyake, K. *et al.* (2013) Efficient and reproducible myogenic differentiation from human iPS cells: prospects for modeling miyoshi myopathy *in vitro*. *PLoS ONE* **8**, e61540.

Vierbuchen, T., Ostermeier, A., Pang, Z.P., Kokubu, Y., Sudhof, T.C. & Wernig, M. (2010) Direct conversion of fibroblasts to functional neurons by defined factors. *Nature* **463**, 1035–1041.

Zhou, Q., Brown, J., Kanarek, A., Rajagopal, J. & Melton, D.A. (2008) *In vivo* reprogramming of adult pancreatic exocrine cells to beta-cells. *Nature* **455**, 627–632.

Received: 17 July 2013
Accepted: 26 November 2013

Supporting Information

Additional Supporting Information may be found in the online version of this article at the publisher's web site:

Figure S1 Categorization of the genes differentially expressed in induced photoreceptor cells from human dermal fibroblasts (CRNO-Fib versus CRN-Fib).

Figure S2 Method for analysis of light responses.

Table S1 List of the enriched GO term (corrected *P*-value < 0.01) for Fig. 4A

Table S2 Up-regulated retina-related genes both in the CRNO-infected fibroblasts and in CRN-infected iris-derived cells (signal ratio ≥ 2.0 for 'up')

SCIENTIFIC REPORTS

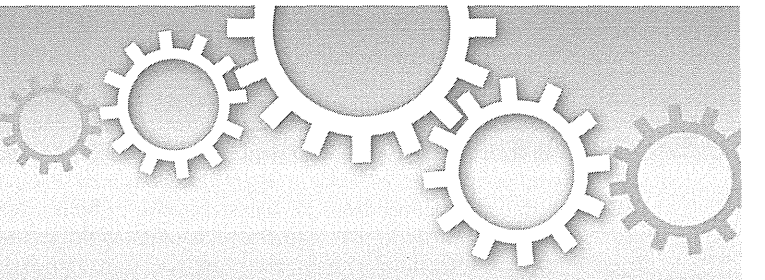

OPEN

SUBJECT AREAS:
RETINA
DIFFERENTIATION
STEM-CELL DIFFERENTIATION

Received
22 September 2014

Accepted
15 January 2015

Published
10 February 2015

Correspondence and requests for materials should be addressed to N.A. (azuma-n@ncchd.go.jp)

* These authors contributed equally to this work.

Generation of retinal ganglion cells with functional axons from human induced pluripotent stem cells

Taku Tanaka[1]*, Tadashi Yokoi[1]*, Fuminobu Tamalu[2], Shu-Ichi Watanabe[2], Sachiko Nishina[1] & Noriyuki Azuma[1]

[1]Department of Ophthalmology and Laboratory of Cell Biology, National Centre for Child Health and Development, Tokyo, Japan, [2]Department of Physiology, Faculty of Medicine, Saitama Medical University, Saitama, Japan.

We generated self-induced retinal ganglion cells (RGCs) with functional axons from human induced pluripotent stem cells. After development of the optic vesicle from the induced stem cell embryoid body in three-dimensional culture, conversion to two-dimensional culture, achieved by supplementation with BDNF, resulted in differentiation of RGCs at a rate of nearly 90% as indicated by a marginal subregion of an extruded clump of cells, suggesting the formation of an optic vesicle. Axons extended radially from the margin of the clump. Induced RGCs expressed specific markers, such as Brn3b and Math5, as assessed using by quantitative PCR and immunohistochemistry. The long, prominent axons contained neurofilaments and tau and exhibited anterograde axonal transport and sodium-dependent action potentials. The ability to generate RGCs with functional axons uniformly and at a high rate may contribute to both basic and clinical science, including embryology, neurology, pathognomy, and treatment of various optic nerve diseases that threaten vision.

Retinal disorders are an important cause of blindness throughout the world[1,2]. Of the various types of retinal cells, photoreceptors and ganglion cells are primarily affected by retinal disorders; photoreceptors are generally affected by retinitis pigmentosa and retinal dystrophy[3,4], while ganglion cells are generally affected by optic neuropathy and glaucoma[5]. Research aimed at achieving regeneration of the diseased retina has identified several candidate structures that contain precursors of key retinal cells, including the iris[6,7], ciliary epithelium[8], and Muller glial cells[9,10]. Two dimensional (2D) cell culture methods have been employed in this work; however, efficient regeneration of photoreceptors and the other retinal cells has not been achieved without application of exogenous factors that relate to retinal morphogenesis[11–13], whereas self-induction by endogenous factors would have been ideal. The establishment of embryonic stem cell (ESC) and induced pluripotent stem cell (iPSC) technologies has recently allowed further advances in the generation of retinal cells.

The development of three-dimensional (3D) culture systems has led to more advanced work on differentiation of neural tissues from ESs and iPSCs, facilitating self-organisation of brain cortical tissue[14], the pituitary gland[15], and the retina starting from mouse and human ESCs[16,17]. First, the optic vesicle and continuous optic cup, which are two early developmental stages of the eyeball, were generated from ESC embryoid bodies. These tissues were then cut with scissors and continuously incubated in a floating culture system under a high-oxygen atmosphere, resulting in self-induction of almost all retinal layers[15,16], including the ganglion cell and photoreceptor cell layers. In further advancements to this method, all layers of the murine retina were generated from ESCs and iPSCs, and retinal sheets were successfully transplanted into the subretinal space of mice with advanced retinal degeneration (rd1), which lacked the outer nuclear layer of the retina[18].

Another series of 3D culture systems has been developed, enabling generation of the 3D retinal structure, including retinal ganglion cell and photoreceptor cell layers. In the primary experiment, adherent human embryonic stem cells and iPS cells were picked up mechanically and transferred to floating culture to be induced into an optic vesicle (OV)-like structure with retinal precursor characteristics. This structure was then reattached to a 2D culture dish, where it differentiated into the retinal cell lineage[19,20]. In subsequent experiments in 3D culture systems, the entire retinal layer, including the retinal ganglion cell layer and functional photoreceptors, was established from human iPSCs mainly using intrinsic cues[21] and addition of small amounts of exogenous factors, as reported in previous studies[22–26]. In this experiment, an OV-like structure was directly differentiated into a retina without the process of optic cup formation. There is a critical difference between these two major

methods; in the former, the OV-like structures were extruded from the embryoid body, while in the latter, aggregates of human iPSCs or ESCs were directly induced into OV-like structures. In both methods[17,21], the entire retinal layer is regenerated, containing thick outer layers with well-differentiated photoreceptors and thin, immature inner layers comprised of RGCs. Moreover, the formation of RGC axons has not been realised using either 3D retinogenesis method.

The RGCs located in the ganglion cell layer of the retina typically have long axons, enabling them to connect the retina to various visual centres in the central nervous system, represented by the lateral geniculate body[27]. RGCs play roles in transmitting image-forming and non-image-forming visual information[28], processed by photoreceptors, horizontal cells, amacrine cells, and bipolar cells, to higher visual centres via converging non-myelinated nerve fibres in the retina that continue into the myelinated optic nerve. Thus, the long axons of RGCs are crucial to transmitting visual images from the retina to the brain.

However, although culture of isolated RGCs with tiny axons from animal and human retinas has been achieved by immunopanning methods[29–31], no study has reported the generation of RGCs exhibiting characteristic long, prominent axons in an *in vitro* culture system, with the exception of one report in which RGCs were developed from mouse iPSCs that carried an Atoh/Math5 lineage reporter[32] and another report in which almost 30% of attached aggregates of RGCs derived from human iPSCs exhibited elongated axons with action potentials[33].

Here, we describe a novel *in vitro* method that generated RGCs with long, functioning axons exhibiting action potentials and axonal transport, by combining cultivation of 3D floating aggregates with a subsequent 2D adhesion culture. This advance may facilitate both basic research on RGCs and translational research aimed at finding treatments for retinal diseases.

Results

Protocol for self-induction of RGCs from human iPSCs. For purposes of generating RGCs, we modified a previously established[17] 3D retinal regeneration protocol (Fig. 1). This method called for addition of both foetal bovine serum (FBS) and Matrigel to the culture medium; these components were not required by other protocols[20,21], which also produced retinal cells efficiently. Therefore, we investigated the effects of FBS concentrations (1%–10%) on D12–18 and Matrigel concentrations (0.5%–2.0%) on D1–18. At all concentrations, embryoid bodies (EBs) were well organised, and OVs, which were maintained over the duration of the study, extruded from nearly 90% of the EBs (Table S1 and Fig. S1). In order to establish RGCs with long axons in a relatively short period, we changed the OV culture conditions from floating (3D) to dish (2D) to obtain cell attachment because the incipient ganglion cell layer was located on the surface of the OV. Initially, we severed the OVs from the EBs, which is predicted to lead to differentiation into neural retinal cells, as demonstrated previously[17]. However, maintenance of the cut OVs did not succeed, as documented in another report[34]. Therefore, we directly attached the OVs to the dish while still connected to the EBs, and the attached OVs were further differentiated into an extruded clump of cells on the dishes. Around 2 days after attachment, massive axonal growth from the margin of the clump was realised. The optimal timing of attachment was also evaluated. Attachment on D26–29 was ideal for elongation of axons from the marginal portion of the clump, which was thought to representthe RGC region (RGCR), while attachment prior to D24 or after D30 seemed suboptimal for efficient development of axons (Fig. S2). When retinoic acid was added 3 days prior to the attachment, axonal growth was promoted (Fig. S3); in contrast, if retinoic acid was continuously supplemented after adhesion, axons grew by around D32, but died back by around D40 (Fig. S4). Finally, following addition of BDNF (100 ng/mL) to promote neuronal survival beyond 3 days of retinoic acid administration, RGCs and their axons were stabilised until around D50 (Fig. S5).

The time course of expression of transcription factors and protein markers associated with retinal development. The OV is derived from the eye field in the forebrain, a process in which several transcription factors, called eye-field transcription factors, play principal roles[35]. The retinal homeobox gene, *Rx*, and the paired box gene 6, *Pax6*, which belong to this group of eye-field transcription factors, are crucial in early retinogenesis[36]. During the period of attachment of the cultured EB with its extruded OV to a dish, temporal gene expression analysis clearly revealed that upregulation of *Rx* began on D6, when the EB had maturely formed, and peaked on D18, when the OVs began to develop. This was followed by upregulation of its downstream target *Pax6*. Math5, the *bHLH* transcription factor, is expressed in post-mitotic retinal precursor cells under direct control by *Pax6*[37]. Math5 crucially regulates RGC formation, and Math5 mutant mice lack RGCs[38,39]. In humans, Math5 mutation results in optic nerve aplasia[40]. Brn3b, known as the most reliable RGC marker, is a member of the POU-domain family of transcription factors, and its expression is controlled by Math5[41]. Brn3b is believed to determine RGC fate by

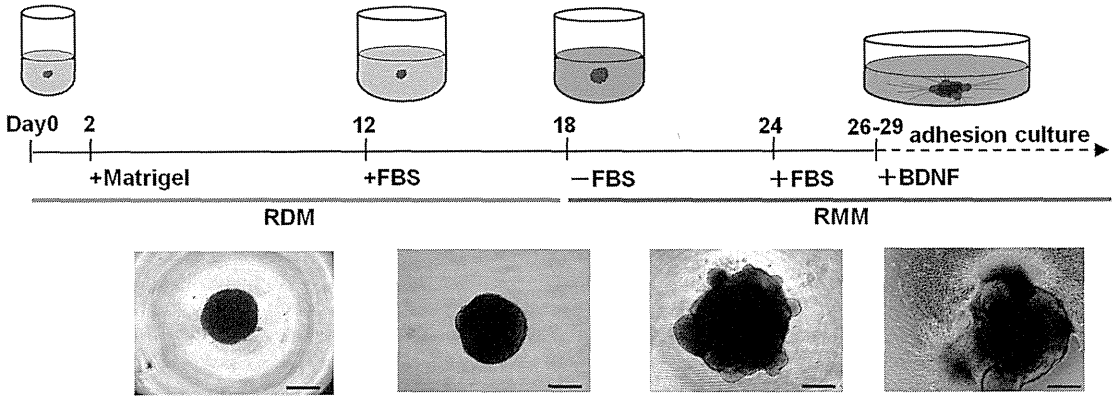

Figure 1 | Schematic diagram of the protocol for self-induction of retinal ganglion cells. This protocol consisted of a period of suspension culture (3D) followed by a period of adhesive culture (2D) and resulted in observation of axonal elongation from retinal ganglion cells (RGCs) from human iPSCs starting within 30 days. Two basal media, retinal differentiation medium (RDM) and retinal maturation medium (RDM) were used. Significant morphological changes occurred after a medium change from RDM to serum-free RMM on D18, at which point optic vesicles (OVs) appeared to extrude from the cultured cell aggregates. Beginning with the start of adhesive culture on D26–29, axons grew out radially from the mass of new RGC bodies. Phase contrast micrographs were taken on D6, D18, D24, and D30 and are shown in sequence from left to right. Scale bar, 500 μm.

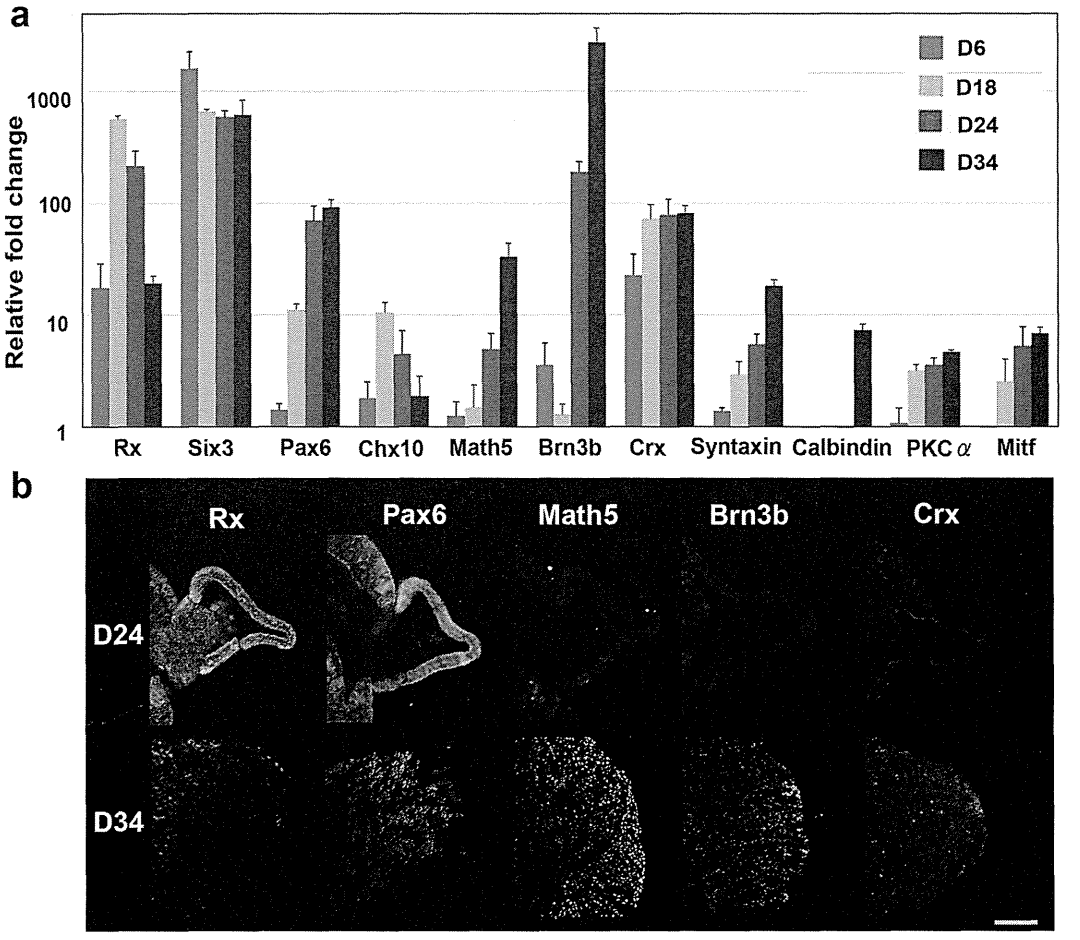

Figure 2 | Commitment of human iPSCs toward a retinal lineage and generation of retinal ganglion cells (RGCs). (a) The time-dependent expression of transcription factors involved in retinogenesis was examined. Expression changes during differentiation of iPSCs to RGCs as revealed by quantitative PCR. Total RNA was extracted on D6, D18, D24, and D34. Retinal progenitor markers, including Rx, Six3, and Pax6, were apparently expressed until D18. Brn3b, the RGC-specific marker, was upregulated in a sporadic manner, following an increase in the expression of Math5, the upstream regulator of Brn3b. Crx, the marker of the cone-rod photoreceptor precursor, could also be identified starting at D18. Syntaxin, the amacrine cell marker, gradually increased following increased Brn3b expression. Expression levels of calbindin, a marker of horizontal cells, and PKCα, a marker of bipolar cells, were quite low. The expression of Mitf, a master controller of retinal pigment epithelium differentiation, was suppressed, indicating that these cells were in the neural retinal lineage. Expression levels of mRNAs were first normalised to the expression of HPRT1 and then to the expression on D0 (the start day of suspension culture), which was set at 1.0. Error bars represent means ± SDs of the samples from three independent experiments. The vertical axis is a base-two logarithmic scale. (b) Immunohistochemistry for Rx, Pax6, Brn3b, Math5, and Crx in the optic vesicle (OV) on the floating EB on D24 and in extrusions of cell clumps that differentiated from the OVs after attachment of the EBs on D34, using each serial section. Rx and Pax6 were expressed in the OV and the extruded clump of cells. Positive immunostaining for Brn3b and Math5, the most specific markers for RGCs, was observed not in the OV, but was observed in the clump and was localised to the outer margin of the clump. Crx, a marker for primitive photoreceptors, was not expressed in the OV but was faintly expressed in the clump. Scale bar, 100 μm.

acting as a repressor of differentiation to non-RGC cell types[42], a process in which Islet1, an LIM-homeodomain factor, acts as a coregulator[43]. In our experiments, expression of Brn3b was relatively low until D18 and then dramatically increased until D24, when the OVs were well developed from the floating EBs following an increase in Math5 expression. Chx10 is associated with the proliferation of retinal progenitor cells. It is initially expressed in all retinal progenitors, but later is restricted to bipolar cells[44]. In our experiments, expression of Chx10 became apparent at D18 and was maintaineduntil at least D34, when RGCs and axons developed after attachment of the EB. *Crx*, a cone-rod-containing gene, shows restricted expression in premature and mature cells of photoreceptor lineage[45,46]. *Crx* expression was also first observed at D18, following Chx10 expression. Amacrine cells start to differentiate immediately after RGC differentiation[47]. In our experiments, syntaxin, an amacrine cell marker[48,49], showed delayed expression following Brn3b expression. The markers associated with horizontal and bipolar cells, both of which develop at later stages of retinogenesis, showed little expression until D34. The time course of gene expression was quite consistent with that in human retinogenesis. Mitf, a microphthalmia-associated transcription factor and the master regulator of melanocyte and retinal pigment epithelium (RPE) development[50], was not highly expressed in the present study, suggesting that our induction protocol induced human iPSCs into the neural retinal lineage but not into the RPE lineage (Fig. 2a).

Immunohistochemistry also showed expression of Rx and Pax6 in both OVs and the clump, while expression of Brn3b and Math5 was observed only in the clump, localised within the margins of the clump. In contrast, low expression ofCrx was observed withinthe clump (Fig. 2b). Calbindin and PKCα were not detected in either the OV or the clump (Fig. S6).

Structure of human iPSC-derived RGCs by light and electron microscopy. We investigated the structure of the RGCs by light

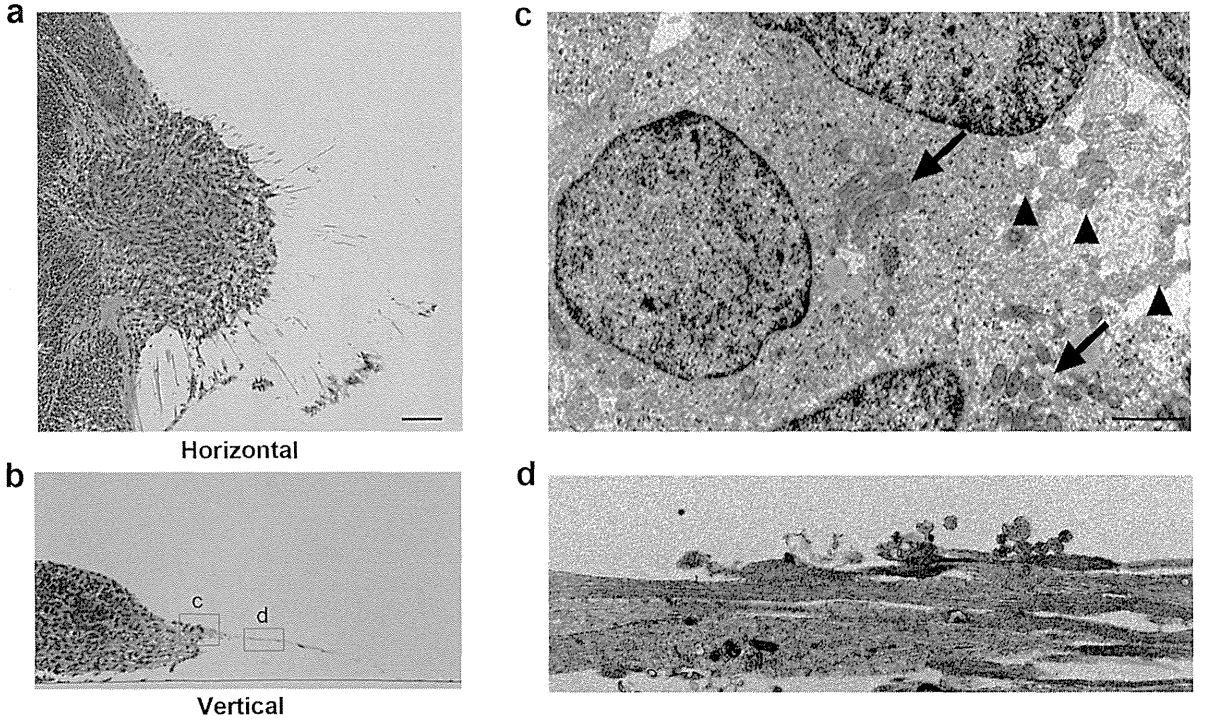

Figure 3 | Light and electron microscopy of induced retinal ganglion cells and their axons. Horizontal (a) and vertical (b) sections stained with haematoxylin and eosin showed that axons radiated from the outer margin of the clump of cells corresponding to the optic vesicle (OV), which extruded from the embryoid body late in 3D culture. Somata of new retinal ganglion cells (RGCs) were present in the marginal portion of the extruded clump and showed variations in size and relatively large nuclei, some of which has Nissl's body characteristics of RGCs, while the main part of the embryoid body (MBEB) contained many irregular rosettes. (c) Electron microscopy analysis of the square portion (c) in panel (b) revealed that cell bodies of RGCs contained prominent rough endoplasmic reticulum (arrows) and that axons (arrowheads) developed from a portion of the axon hillock. (d) Electron microscopy analysis of the square portion (d) in panel (b) revealed straight axons of varied calibre, ranging in diameter from 0.5 to 2 μm and lacking myelination. The axons contained numerous neurotubules. Scale bars, 80 μm in panels (a) and (b); 5 μm in panels (c) and (d).

and electron microscopy. After the OV became attached around D26–29, it became complanate, filled with cells, and showed radiation of numerous axons from the outer margin at the dish surface. The cells in the clump were apparently different from those in the main body of the EB, which was filled with small round cells. The cells in the clump showed relatively large cell bodies (range: 16.1–23.6 μm; average: 21.6 μm, n = 10) with clear cytoplasms and nuclei and spindle-shaped or round cell bodies, sometimes accompanied by a prominent axon. These findings were identical to those of RGCs *in vivo*, whose cell body sizes ranged from 12 to 25 μm[51]. Notably, several cells located peripheral to the structure had Nissl bodies (Fig. S7), which is considered characteristic of RGCs[52]. However, Nissl bodies were not detected in other types of cells, including those in rosettes. The axons were eosinophilic, had few branches, and grew radially from the clump (Fig. 3a, b).

Electron microscopy of D35 specimens demonstrated that the RGCs, which had axons, seemed to be relatively large (range: 16.0–24.1 μm; average: 20.6 μm, n = 10) and were stratified at the margin of the clump. These RGCs contained prominent rough endoplasmic reticulum, which represented the Nissl bodies that were observed by light microscopy. The axons developed from the axon hillock, which exhibited a characteristic conical cell body with neurotubules but no rough endoplasmic reticulum (Fig. 3c), which have also been detected in RGCs *in vivo*[53,54] and define the end of the soma of neurons. The axons contained numerous neurotubules. The diameters of the axons varied (range: 1.7–2.2 μm; average: 1.8 μm, n = 10), and the axons were not myelinated (Fig. 3d). These findings were identical to those of axons in the retinal nerve fibre layer and in the optic nerve anterior to the lamina cribrosa, whose diameters range from 0.6 to 2.0 μm[51].

Determination of RGC lineages. To confirm that the cells with axons in the margin of the clump differentiated from the OV were RGCs, we examined the expression and distribution of typical markers associated with RGCs. Real-time PCR revealed a more than 30-fold increase in the expression of Brn3b, Math5, Islet1, γ-synuclein (Sncg), and Tuj1. Brn3b, the most specific marker in this group, showed a nearly 3,000-fold increase in expression at D34 compared with D1 (Fig. 4a). Immunohistochemistry showed positive staining for all markers except Tuj1 in the marginal portion of the clump, which was therefore thought to be the incipient RGC layer. Math5, an upstream transcription factor for Brn3b, and Sncg, another RGC marker and contributor to neurofilament integration[55], showed similar distributions in the marginal portion of the clump. Islet1, a marker of RGCs and amacrine cells, was positive both in the margin and further toward the interior of the clump, suggesting that amacrine cells also developed there. Notably, Brn3b-positive cells apparently localised to the outermost margin of the clump at the surface of the dish, which strongly indicated that the margin was the RGCR and that the long radial axons originated from the RGCR. The costaining of Brn3b and Tuj1 demonstrated that the axons originated from the Brn3b-positive cells (Fig. 4b).

Sectional gene expression associated with RGCs and other retinal cells. For further confirmation of the presence of localised RGCs in the supposed RGCR, we mechanically divided the adherent structural complex into three parts: the RGCR, OVR, and MBEB (Fig. 5a). Notably, Brn3b showed nearly four-fold higher expression in the RGCR than that in the MBEB. In addition, Crx expression was strongly suppressed in the RGCR. These results obviously demonstrated that the RGCR was highly specified into

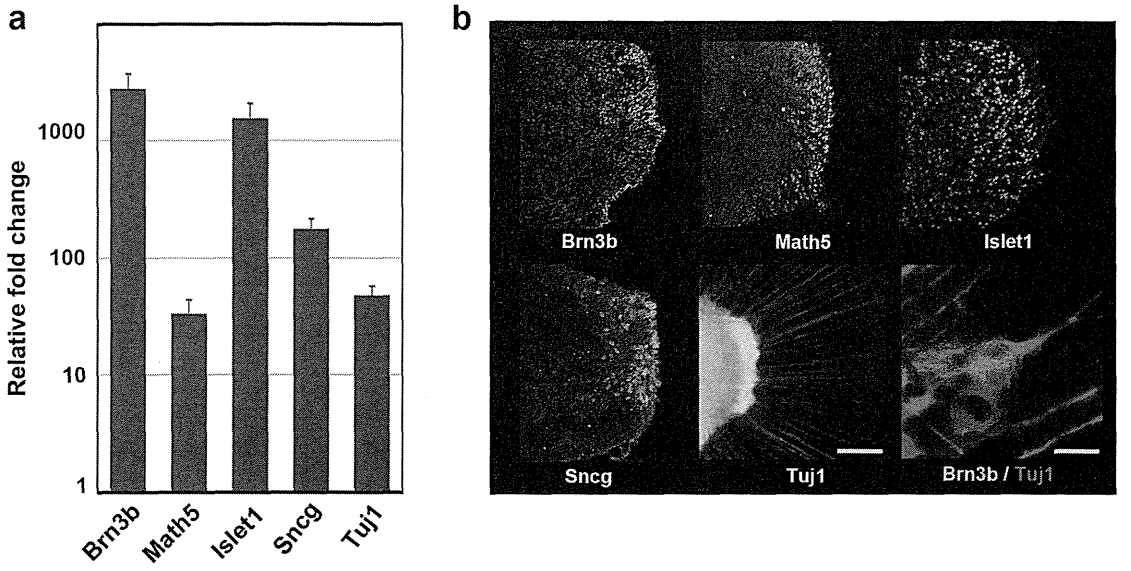

Figure 4 | Expression of characteristic markers related to retinal ganglion cells. The expression levels of representative retinal ganglion cell (RGC) markers, Brn3b, Math5, Islet1, γ-synuclein (Sncg), and β3-tubulin (Tuj1), were examined. (a) Quantitative PCR analysis of total RNA extracted on D34 was used. All markers associated with the RGC lineage were obviously upregulated more than 30-fold. In particular, the mRNA levels of Brn3b and Islet1 were increased dramatically. The mRNA expression levels were first normalised to HPRT1 expression and then to mRNA expression on D0. Error bars represent means ± SDs of three samples. The vertical axis was a base-two logarithmic scale. (b) Immunohistochemistry for Brn3b, Math5, Islet1, Sncg, and Tuj1 on D34. Whole mount staining for Tuj1 and serial section staining for the other targets were analysed. Positive immunostaining for Brn3b and Math5, the most specific markers for RGCs, was localised to the outer margin of the extrusion that differentiated from the optic vesicle. Sncg, a marker for RGCs, and Islet1, a marker for RGCs and amacrine cells, were expressed in the inner part of the clump. Axons were strongly positive for Tuj1, and the axons were confirmed to grow from Brn3b-positive cells. Scale bar, 100 μm. Scale bar for the double staining of Brn3b and Tuj1, 10 μm.

the ganglion cell lineage. Islet1 (a marker for ganglion and amacrine cells) was also up regulated in both the RGCR and OVR, which was consistent with the distribution of Islet1 expression confirmed by immunostaining (Fig. 5b). We also noticed that the isolated RGCR survived for approximately 10 days after separation from the OVR, which suggests that mechanical purification of RGCs is possible after growth of abundant axons.

RGC axon-related protein expression and determination of types of neurofilament proteins in early retinal gangliogenesis. To confirm that the apparent axons emanating from the RGCR resembled typical axons, we used tau and neurofilament (NF) immunostaining (Fig. 6b). The time-series expression of all NF components—neurofilament-light (NFL), neurofilament-medium (NFM), and neurofilament-heavy (NFH)—was studied in parallel

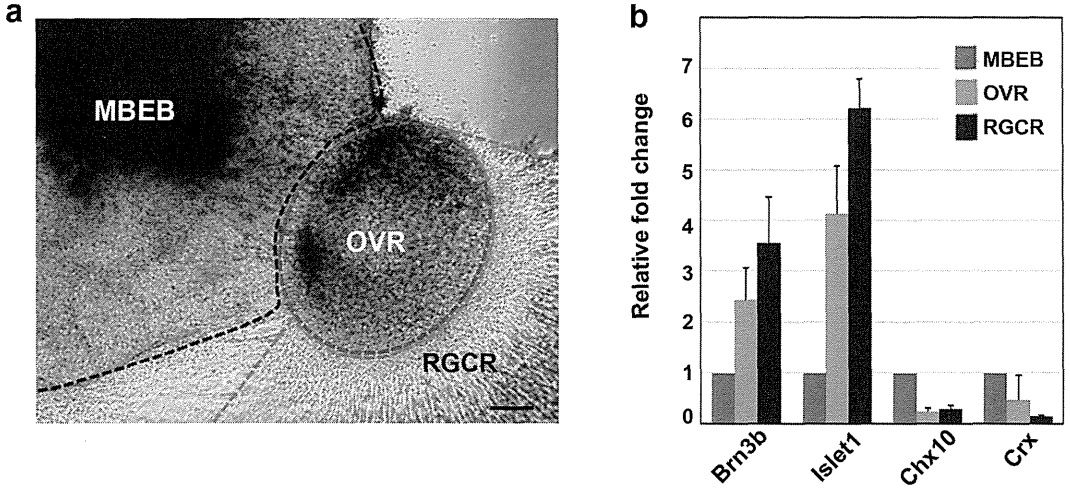

Figure 5 | Regional differentiation of retinal ganglion cells detected by RT-PCR. (a) Each colony on D34 was mechanically divided into three regions, namely the main body of the embryoid body (MBEB), the extruded clump of cells differentiated from the optic vesicle except for its marginal part (OVR; optic vesicle region), and the retinal ganglion cell region (RGCR). The latter was comprised of the marginal layer of the extrusion and the axons. (b) The gene expression of neural retinal markers in each region was investigated by quantitative PCR analysis. Analysed markers included Brn3b (RGCs), Islet1 (RGCs, amacrine cells), Crx (photoreceptors), and Chx10 (neural retina progenitor and bipolar cells). The RGCR showed high expression of Brn3b compared with the other two regions, but lacked Crx expression, suggesting that the RGCR was specifically differentiated into the RGC lineage. The mRNA expression levels were first normalised to HPRT1 expression and then to mRNA expression levels on D0. Error bars represent means ± SDs of three samples from three independent experiments. Scale bar, 100 μm.

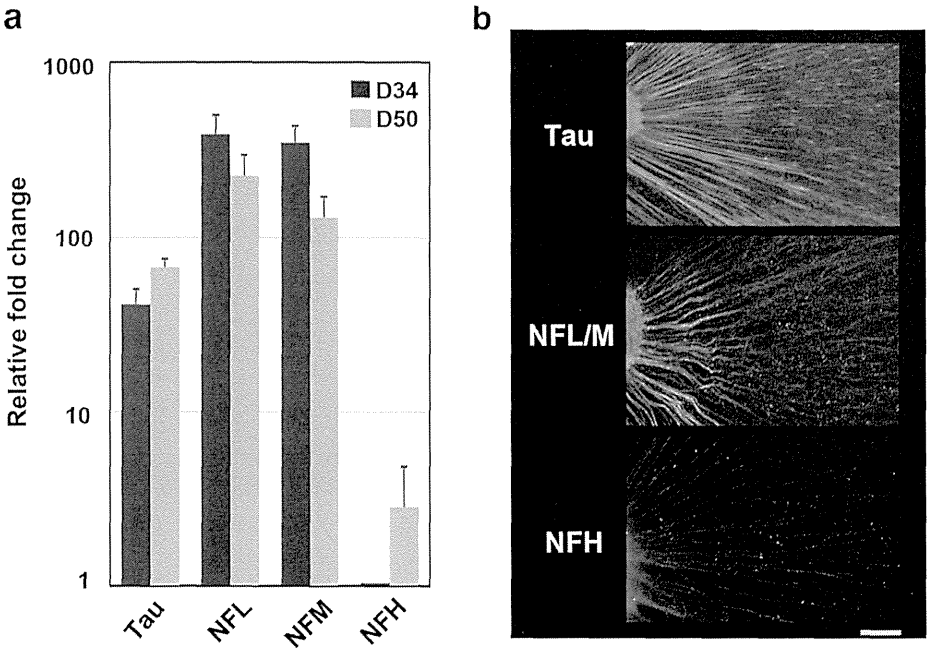

Figure 6 | Cytoskeleton in axons elongated from retinal ganglion cells. (a) Quantitative PCR analysis was applied to investigate nerve fibre markers, including neurofilament (NF) light (NFL), NF middle (NFM), NF heavy (NFH), and tau, using total RNA extracted on D34 and D50. The expression of each marker, including NFL, NFM, and tau, was already high at D34, while that for NFH was increased on D50 compared with D34, probably a reflection of axonal maturation. (b) Immunohistochemistry clearly showed positive staining in all axons for NFL, NFM, and tau at D34 and D50 and for NFH at D50. The mRNA expression levels were first normalised to HPRT1 expression and then to the mRNA expression levels of NFH on D34. Scale bar, 100 μm.

(Fig. 6a). Microtubules, NFs, microtubule-associated proteins (MAPs), and actin play crucial roles in axonal development[56]. Tau, which is a MAP, contributes to polymerisation, stabilisation, and organisation of microtubules and promotes axonal growth and effective axonal transport[57]. Once tau is hyperphosphorylated, the axonal transport process and cell survival of RGCs are compromised[58]. The axons detected in our study were clearly stained for tau and associated with evidence of axonal transport. NFs are the intermediate filaments of neurons and are especially abundant in CNS axons, where they occur as heteropolymers made up of four subunits, namely NFL, NFM, NFH, and α-internexin[59]. NFs have essential roles in radial axonal growth and maintenance of axon calibre, therefore mediating the ability to transmit action potentials[60]. Both NFL and NFM appear early in retinogenesis, while synthesis of NFH is delayed[61]. In our experiments, NFL and NFM were already highly expressed at D34 and expression continued until D50, while expression of NFH was quite low at D34 and gradually increased until D50. Specimens from D34 showed positive staining for NFL/M but weak staining for NFH, in agreement with the expression time series study. We observed temporally varying gene expression not only of transcription factors but also of genes associated with structural components of RGCs.

Axonal transport in human iPSC-derived RGCs. To establish axonal function, we tested for axonal transport in the apparent axons that radiated from the RGCR. Axonal transport showed two characteristic flows, slow and fast, both of which had anterograde and retrograde components. RGCs and their axons are known to be rich in mitochondria and to maintain homeostasis by axonal transport, as in other neurons. Neurotrophic tyrosine kinase receptor 1 (NTRK1), a member of the neurotrophic tyrosine kinase receptor family, is the receptor for nerve growth factor and is expressed in RGCs, especially when the cells are damaged[62–64]. Using NTRK1 and mitochondria as tracers, we directly introduced plasmid vectors composed of GFP-NTRK1 with a CMV promoter and mCherry-mitochondria with a CMV promoter into the cell body of RGCs around D34 by electroporation to analyse anterograde rapid axonal transport. Several axons demonstrated anterograde axonal transport after approximately 7–10 h post-introduction. The cell bodies corresponding to these axons expressed these factors as well (Fig. 7a).

To detect a time series of axonal transport, Alexa-Fluo-555 conjugated cholera toxin B, which is also known as a tracer of axonal transport[58], was administrated. Slow and fast anterograde axonal flow were clearly observed by injection of the toxin into RGCR (Fig. 7b, Fig. S8, Supplemental Video 1). The transport was blocked by an addition of 1 mM colchicine (Fig. S9, Supplemental Video S2 and S3).

Human iPS cell-derived RGCs showed neuronal excitability. To determine whether iPSC-derived RGCs could generate action potentials, we examined the RGCs in the RGCR (Fig. 8a). The RGCs each had a long axon process extending to the filter paper side and possessed some dendritic processes (Fig. 8b). Electrophysiological analysis of cells with an axon process revealed repetitive action potentials in response to current injection through the recording pipette in current clamp mode (4 of 5 cells; Fig. 8c). The resting membrane potential and the amplitude of the first action potential were -81.8 ± 26.8 mV and 56.8 ± 24.6 mV, respectively ($n = 4$). The cells that generated action potentials exhibited tetrodotoxin (TTX)-sensitive sodium-dependent currents with a maximum amplitude of $1{,}248 \pm 573$ pA ($n = 4$), followed by outward currents (Fig. 8d).

Discussion

In this study, we generated RGCs with functioning axons from human iPSCs. The present quantitative PCR and immunohistochemistry results showed a gene expression profile and protein markers characteristic of RGCs, including Brn3b, Math5, Islet1, Sncg, and Tuj1. RGCs induced from ESCs and iPSCs in previous studies carried markers characteristic of RGCs[17,21,65], but were not accompanied by long axons. RGCs have also been generated in 3D culture